Chapter 3

A minimal inverse seesaw model with S_4 flavour symmetry

We present a minimal inverse seesaw model with S_4 flavour symmetry. The model extends the standard model by including two right-handed and two standard model gauge singlet neutrinos to explain the small masses of neutrinos. The model accurately describes lepton mass spectra and flavour mixing for normal hierarchy of neutrino masses. The prediction of the model on the Dirac CP-violating phase is centered around 370.087°. Furthermore, we calculated the effective Majorana neutrino mass, $|\langle m_{ee}\rangle|$, which is associated with neutrinoless double beta decay within the allowed region of the model parameters.

3.1 Introduction

It has been established through various experiments [1–4] that neutrinos have mass and their flavors are mixed. However, according to the Standard Model (SM), neutrinos are considered to be massless. This suggests that there is physics beyond the SM. There are various theories that can explain the origin of tiny neutrino masses. The seesaw mechanism [5–9], radiative seesaw mechanism [10], and models based on extra dimensions [11, 12] are some of them. One such framework is the inverse seesaw (ISS) mechanism. In this mechanism, the SM is

extended by introducing SM gauge singlets and right-handed (RH) neutrinos [13, 14]. In contrast to the canonical seesaw mechanism, the ISS mechanism involves the heaviness of right-handed neutrinos as well as a small lepton-number violating mass parameter, here denoted by μ. These parameter causes the suppression of the neutrino mass, which in turn allows for lighter right-handed neutrinos (TeV-scale) and $\mathcal{O}(1)$ Yukawa coupling. The gauge-invariant Lagrangian of the extension of the SM can be written as

$$-\mathcal{L}_\nu = Y_\nu \bar{l}_L \tilde{H} N_R + M_R \left(\bar{N}_R\right)^c (S_L)^c + \frac{1}{2}\mu \bar{S}_L (S_L)^c + h.c., \tag{3.1}$$

where l_L is the left-handed doublet, H is the Higgs doublet,$\tilde{H} = i\sigma_2 H^*$ with σ_2 being the 2^{nd} Pauli matrix, N_R are the right-handed neutrino singlets and S_L are the SM gauge singlets. After the Higgs doublet, H acquires vacuum expectation value (vev), i.e., $\langle H \rangle = v = 174$ GeV and breaks the gauge symmetry, the neutrino mass matrix may be written as

$$M_\nu = \begin{pmatrix} 0 & m_D & 0 \\ m_D^T & 0 & M_R \\ 0 & M_R^T & \mu \end{pmatrix}, \tag{3.2}$$

where $m_D = Y_\nu v$ is the Dirac mass matrix, M_R is a complex matrix and μ is a complex, symmetric matrix. With $\mu << m_D << M_R$, diagonalisation of equation (3.1) lead to

$$m_\nu = m_D \left(M_R^T\right)^{-1} \mu \left(M_R\right)^{-1} m_D^T. \tag{3.3}$$

In the ISS model, with the $\mathcal{O}(m_D) \sim 10^2$ GeV, the mass of light neutrinos $\mathcal{O}(m_\nu) \sim 0.1$ eV may be suppressed by the smallness of μ with $\mathcal{O}(\mu) \sim 10^3$ eV as well as the heaviness of right-handed neutrino masses $\mathcal{O}(M_R) \sim 10^4$ GeV. The heavy neutrinos have a slightly lower mass scale than the canonical seesaw model. This makes them potentially testable at future colliders. Another aspect of the flavour structure of the SM is the observed fermion mixing. For the lepton sector, experimental evidence shows two large and a small mixing angles, however, the origin of such mixing patterns is still unanswered. The answer to such

a problem can be given by introducing non-Abelian discrete flavour symmetries into the Lagrangian of the model [15–17]. Various models based on A_4 [18–25], S_4 [26–39], A_5 [40, 41], etc. have been proposed over the years to explain the observed lepton flavour mixing pattern. In models based on non-Abelian discrete symmetries, the discrete symmetry which is exact at a high-energy scale breaks down distinctly leaving residual symmetry in the charged-lepton and neutrino sectors at low-energy scales. This breaking pattern is governed by the *vev* of the scalar field known as flavons (singlets under SM gauge symmetry) and eventually determines the lepton flavour mixing pattern.

In the work presented in this chapter we investigate the ISS model with S_4 flavour symmetry and analyze its ability to account for neutrino masses, mixing, and CP violation. We work in the framework with minimal ISS(2, 2) which is the minimal possible form of ISS mechanism that can account for the neutrino mass spectra [42]. The resulting neutrino mass matrix is tested against the neutrino experimental data using chi-squared analysis. We further explore the implications of the model for neutrinoless double beta decay.

The rest of the chapter is structured as follows. In section 3.2, we construct the S_4 flavour symmetric inverse seesaw model with two right-handed and two SM gauge singlet neutrinos. Section 3.3 includes the numerical analysis and the results of the model presented in section 3.2. We investigate the viability of the model to explain the latest data from neutrino oscillation experiments using chi-squared analysis. Further, we define the allowed region of the parameters of the model corresponding to $\chi^2 \leq 30$ values. This section also includes the results on neutrinoless double beta decay predicted by the model and we finally summarise our conclusions in section 3.4. In Appendix B we give a brief description of the S_4 group. The scalar sector and details of the vacuum alignments are included in Appendix B.

3.2 The Model

We consider the extension of the SM by including additional S_4 flavour symmetry. It is further augmented with $Z_3 \times Z_4$ group to achieve the desired structures for the mass matrices. The fermion sector of the model includes the addition of two right-handed neutrinos and two SM gauge singlet fermions to the SM fermion content, resulting in ISS(2, 2) framework. In the scalar sector, we have one $SU(2)_L$ Higgs doublet H, and $SU(2)_L$ singlet flavons ϕ_c, φ_c, ϕ_ν, χ, ψ. Table 3.1 presents the transformation properties of the various fields of the model under different symmetry. The Yukawa Lagrangian which is invariant under the flavour symmetry, is of the form

$$\begin{aligned} -\mathcal{L} \supset & \frac{\alpha_1}{\Lambda}\bar{l}_L H\varphi_c e_R + \frac{\alpha_2}{\Lambda}\bar{l}_L H\varphi_c(\mu_R,\tau_R) + \frac{\alpha_3}{\Lambda}\bar{l}_L H\phi_c(\mu_R,\tau_R) \\ & + \frac{\beta_1}{\Lambda}\bar{l}_L\tilde{H}\varphi_\nu N_R + \gamma_1\bar{N}_R\xi S_1 + \gamma_2\bar{N}_R\xi S_2 + \lambda_1 S_1 S_1\psi + \lambda_2 S_2 S_2\psi + h.c., \end{aligned} \tag{3.4}$$

where α_1, α_2, α_3, β_1, γ_1, γ_2, λ_1, and λ_2 are the Yukawa coupling constant.

The *vev* of the flavons in the charged-lepton sector are $\langle\varphi_c\rangle = (v_{\varphi_c}, 0, 0)$, $\langle\phi_c\rangle = (v_{\phi_c}, 0, 0)$ [43]. The charged-lepton mass matrix obtained after flavour and electroweak symmetry breaking is of the form,

$$m_l = \frac{v}{\Lambda}\begin{pmatrix} \alpha_1 v_{\varphi_l} & 0 & 0 \\ 0 & \alpha_2 v_{\varphi_l} + \alpha_3 v_{\phi_l} & 0 \\ 0 & 0 & \alpha_2 v_{\varphi_l} - \alpha_3 v_{\phi_l} \end{pmatrix}. \tag{3.5}$$

The hierarchy of charged leptons can be explained using the Froggatt-Nielsen mechanism, following the approach presented in [43]. For the neutrino sector, we assume that the flavons develop *vev* in a region of the scalar potential's parameter space where[1]

$$\langle\varphi_\nu\rangle = (v_{\varphi_{\nu_1}}, v_{\varphi_{\nu_2}}, v_{\varphi_{\nu_3}}), \quad \langle\xi\rangle = (v_\xi, v_\xi), \quad \langle\psi\rangle = v_\psi. \tag{3.6}$$

After electroweak gauge and flavour symmetry breaking, we get the following

[1]The details of the scalar sector and vacuum alignments are shown in appendix **Appendix**.

Field	l_L	e_R	(μ_R, τ_R)	H	N_R	S_1	S_2	φ_c	ϕ_c	φ_ν	ξ	ψ
$\mathbf{S_4}$	3_1	1_1	2	1_1	2	1_1	1_2	3_1	3_2	3_1	2	1_1
$\mathbf{Z_3}$	1	ω^2	ω^2	ω	1	1	1	1	1	ω	1	1
$\mathbf{Z_4}$	i	1	1	1	i	i	i	i	i	1	1	-1

Table 3.1: Field content of the model and their charge assignment under $S_4\times$ $Z_3\times Z_4$.

matrices for the mass term and couplings

$$m_D = \begin{pmatrix} b & c \\ a & b \\ c & a \end{pmatrix}, \quad M_R = \begin{pmatrix} d & d \\ d & -d \end{pmatrix}, \quad \mu = \begin{pmatrix} e & 0 \\ 0 & e \end{pmatrix}, \tag{3.7}$$

where $a = \frac{\beta_1}{\Lambda} v v_{\varphi_{\nu_1}}$, $b = \frac{\beta_1}{\Lambda} v v_{\varphi_{\nu_2}}$, $c = \frac{\beta_1}{\Lambda} v v_{\varphi_{\nu_3}}$, $d = \gamma_1 v_\xi \simeq \gamma_2 v_\xi$, and $e = \lambda_1 v_\psi \simeq \lambda_2 v_\psi$.

Using the matrices of equation (3.7) in the inverse seesaw formula (equation (3.3)), the light neutrino mass matrix becomes

$$m_\nu = m_0 \begin{pmatrix} 1+\beta^2 & \alpha+\beta & \beta(1+\alpha) \\ \alpha+\beta & 1+\alpha^2 & \alpha(1+\beta) \\ \beta(1+\alpha) & \alpha(1+\beta) & \alpha^2+\beta^2 \end{pmatrix}, \tag{3.8}$$

where we have defined two complex dimensionless parameters $\alpha = a/b$, $\beta = c/b$ and the factor m_0 denotes the mass scale. The light neutrino mass matrix of equation (3.8) is diagonalized by the Pontecorvo-Maki-Nakagawa-Sakata (PMNS) mixing matrix, $U_{\rm PMNS}$

$$U^\dagger_{\rm PMNS} m_\nu U^*_{\rm PMNS} = {\rm diag}(m_1, m_2, m_3), \tag{3.9}$$

with m_1, m_2, and m_3 being the mass eigenvalues. In standard PDG parametriza-

tion, the PMNS mixing matrix is given by

$$U_{\text{PMNS}} = \begin{pmatrix} c_{12}c_{13} & s_{12}c_{13} & s_{13}e^{-i\delta_{CP}} \\ -s_{12}c_{23} - c_{12}s_{23}s_{13}e^{i\delta_{CP}} & c_{12}c_{23} - s_{12}s_{23}s_{13}e^{i\delta_{CP}} & s_{23}c_{13} \\ s_{12}c_{23} - c_{12}c_{23}s_{13}e^{i\delta_{CP}} & -c_{12}s_{23} - s_{12}c_{23}s_{13}e^{i\delta_{CP}} & c_{23}c_{13} \end{pmatrix} P_M, \tag{3.10}$$

where,

$$P_M = \begin{pmatrix} e^{i\rho} & 0 & 0 \\ 0 & e^{i\sigma} & 0 \\ 0 & 0 & 1 \end{pmatrix}. \tag{3.11}$$

In the model under study, the lightest neutrino mass $m_1(m_3)$ is zero in the case of the Normal Hierarchy (Inverted Hierarchy) of neutrino masses. It is worth noting that for $m_1 = 0$ (NH), the Majorana CP phase ρ is zero and in the case of IH with $m_3 = 0$ the phases can be redefined as $(\sigma - \rho) \to \sigma$. Thus, the model has a single Majorana CP phase and the phase matrix effectively becomes $P_M = diag(1, e^{i\sigma}, 1)$.

3.3 Numerical Analysis and Results

As discussed in the previous section, we have considered the extension of SM by including two RH neutrinos and two SM gauge singlets resulting in a framework known as the ISS(2,2) model. We have shown how S_4 flavour symmetry can be implemented in such a framework and we have obtained the light neutrino mass matrix as shown in equation (3.8). The neutrino mass matrix of equation (3.8) contains four real parameters (Re(α), Im(α), Re(β), Im(β)) that effect the neutrino mixing matrix elements. In this section, we will perform a numerical analysis to test the model against the experimental data. We proceed by writing the neutrino oscillation parameters (θ_{12}, θ_{23}, θ_{13}, Δm^2_{21}, $\Delta m^2_{31(32)}$, δ_{CP}) in terms of the model parameters and scrutinize the ability of the model to explain the neutrino experimental data [44].

Using the light neutrino mass matrix we can define the hermitian matrix, $h_\nu = m_\nu m_\nu^\dagger$ such that

$$h_\nu = m_0^2 \begin{pmatrix} A & B & C \\ B^* & D & E \\ C^* & E^* & F \end{pmatrix}, \tag{3.12}$$

with,

$$\begin{aligned}
A =& |1+\beta^2|^2 + |\alpha+\beta|^2 + |\beta(1+\alpha)|^2 \\
B =& (1+\beta^2)(\alpha+\beta)^* + (\alpha+\beta)(1+\alpha^2)^* + (\beta+\alpha\beta)(\alpha+\alpha\beta)^* \\
C =& (1+\beta^2)(\beta+\alpha\beta)^* + (\alpha+\beta)(\alpha+\alpha\beta)^* + (\beta+\alpha\beta)(\alpha^2+\beta^2)^* \\
D =& |(\alpha+\beta)|^2 + |(1+\alpha^2)|^2 + |(\alpha+\alpha\beta)|^2 \\
E =& (\alpha+\beta)(\beta+\alpha\beta)^* + (1+\alpha^2)(\alpha+\alpha\beta)^* + (\alpha+\alpha\beta)(\alpha^2+\beta^2)^* \\
F =& |\beta(1+\alpha)|^2 + |(\alpha+\alpha\beta)|^2 + |(\alpha^2+\beta^2)|^2.
\end{aligned}$$

The analytical relations between the elements of the hermitian matrix h_ν and the three mixing angles as well as the Dirac CP-violating phase can be written as [45]

$$\begin{aligned}
\tan\theta_{23} &= \frac{Im(B)}{Im(C)} \\
\tan 2\theta_{12} &= \frac{2N_{12}}{N_{22}-N_{11}} \\
\tan\theta_{13} &= |Im(E)| \cdot \frac{\sqrt{\{[Im(B)]^2 + [Im(C)]^2\}^2 + G^2}}{\sqrt{\{[Im(B)]^2 + [Im(C)]^2\}J^2}} \\
\tan\delta_{CP} &= -\frac{[Im(B)]^2 + [Im(C)]^2}{G},
\end{aligned} \tag{3.13}$$

where the quantities N_{11}, N_{12}, and N_{22} is expressed as

$$\begin{aligned}
N_{11} &= A - \frac{J}{Im(E)} \\
N_{12} &= \left[\frac{J^2}{[Im(B)]^2 + [Im(C)]^2} + \left[\frac{G^2}{\{[Im(B)]^2 + [Im(C)]^2\}^2} + 1\right][Im(E)]^2\right]^{\frac{1}{2}} \\
N_{22} &= \frac{[Im(C)]^2 D + [Im(B)]^2 F - 2Im(B)Im(C)Re(E)}{[Im(B)]^2 + [Im(C)]^2}
\end{aligned} \tag{3.14}$$

Parameter	Best-fit $\pm 1\sigma$	3σ range
$\sin^2\theta_{12}$	$0.304^{+0.013}_{-0.012}$	0.269 - 0.343
$\sin^2\theta_{23}$ (NH)	$0.573^{+0.018}_{-0.023}$	0.405 - 0.620
$\sin^2\theta_{23}$ (IH)	$0.578^{+0.017}_{-0.021}$	0.410 - 0.623
$\sin^2\theta_{13}$ (NH)	$0.02220^{+0.00068}_{-0.00062}$	0.02034 - 0.02340
$\sin^2\theta_{13}$ (IH)	$0.02238^{+0.00064}_{-0.00062}$	0.02053 - 0.02434
$\frac{\Delta m^2_{21}}{10^{-5}\mathrm{eV}^2}$	$7.42^{+0.21}_{-0.20}$	6.82 - 8.04
$\frac{\lvert\Delta m^2_{3l}\rvert}{10^{-3}\mathrm{eV}^2}$ (NH)	$2.515^{+0.028}_{-0.028}$	2.431 - 2.599
$\frac{\lvert\Delta m^2_{3l}\rvert}{10^{-3}\mathrm{eV}^2}$ (IH)	$2.498^{+0.028}_{-0.029}$	2.584 - 2.413

Table 3.2: Latest experimental data on neutrino oscillation considered in our analysis [44].

and,

$$G = Re(B)Im(B) + Re(C)Im(C)$$
$$J = Re(B)Im(C) - Im(B)Re(C)$$

It is clear that for a specific point in the four-dimensional parameter space of the model, there is a certain value of the experimental observables given by equation (3.2). Consequently, any variation in the model parameters changes the value of the neutrino oscillation parameters resulting from the model. In order to test the model against the latest experiment data on neutrino mixing parameters, we define a χ^2-function and perform a numerical simulation using a sampling package `MultiNest` [46]. The χ^2-function used in our analysis has the following form

$$\chi^2 = \sum_i \left(\frac{P_i(p) - P_i^0}{\sigma_i} \right)^2 , \tag{3.15}$$

where $P_i(p)$ is the value of the observables predicted by the model at a point p in the four-dimensional parameter space of the model, P_i^0 and σ_i denotes the central value, and the corresponding 1σ error of the i^{th} experimental observable. The ex-

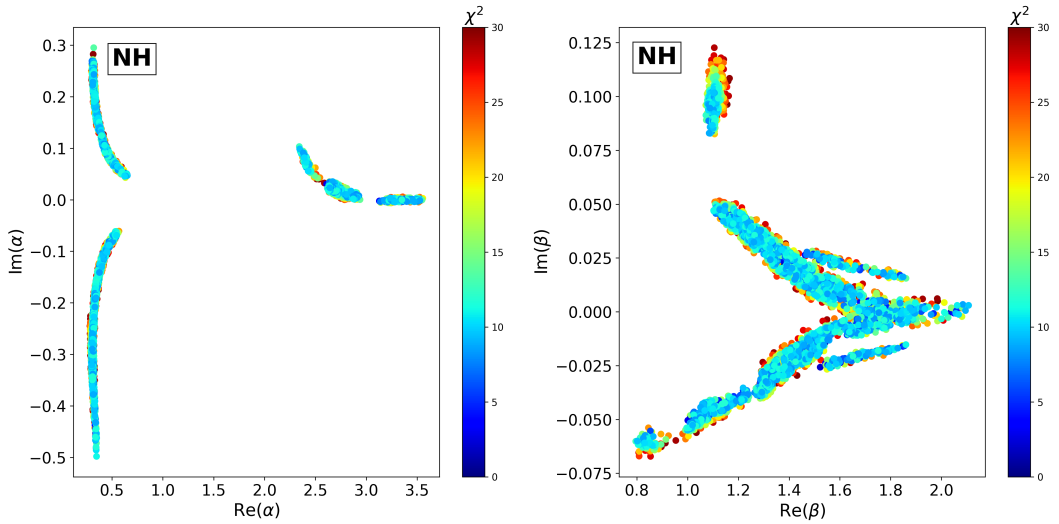

Figure 3.1: Allowed region for the model parameters $Re(\alpha)$, $Im(\alpha)$, $Re(\beta)$, and $Im(\beta)$.

perimental values of the neutrino observables used in our analysis are summarised in Table 3.2. In equation (3.15), we do not consider the Dirac CP-violating phase δ_{CP} as an input. The reason is the weak statistically preferred value of maximally violating CP phase from global experimental data. To carry out the test we treat the parameters of the model to be free and allow them to randomly vary in the following range

$$Re(\alpha),\ Im(\alpha),\ Re(\beta),\ Im(\beta) \in [-10, 10]. \tag{3.16}$$

The values for the three mixing angles and the Dirac CP violating phase can be obtained using equation (3.13). The best-fit values of the model parameter correspond to the minimum value of χ^2. We found that the model provides a good description of the experimental data for NH of neutrino masses with a minimum chi-squared value of approximately 0.24. However, it fails to describe the data for IH where the minimum chi-squared value is greater than 100. The figure 3.1 displays the allowed region of the model's parameter space. The colors represent the range of values for χ^2. Here, we have shown the values of the parameters of the model corresponding to $\chi^2 \leq 30$. The best-fit values of the model parameters

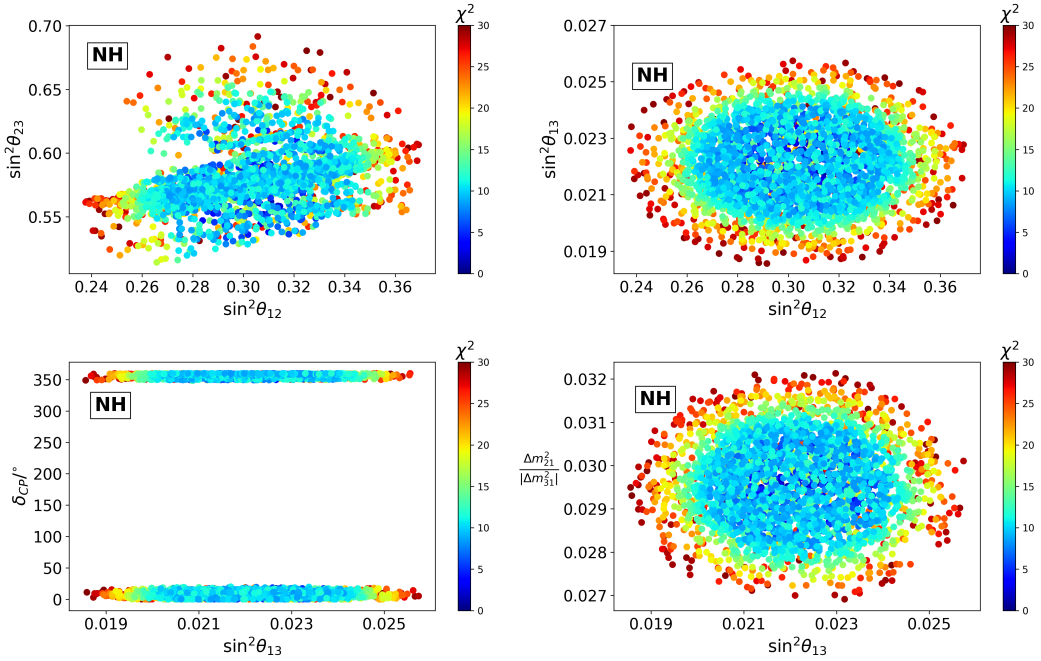

Figure 3.2: Correlation between the neutrino oscillation parameters with the color indicating the ranges of χ^2 values.

$\sin^2\theta_{12}$	$\sin^2\theta_{23}$	$\sin^2\theta_{13}$	$\delta_{CP}/^\circ$	Δm^2_{21} (eV^2)	Δm^2_{31} (eV^2)
0.303	0.575	0.0225	370.087	7.42×10^{-5}	2.510×10^{-3}

Table 3.3: The best-fit values for the neutrino oscillation parameters from χ^2 analysis.

obtained by minimizing the χ^2-function are $Re(\alpha) = 0.314$, $Im(\alpha) = -0.255$, $Re(\beta) = 1.293$, and $Im(\beta) = 0.032$ in NH [2]. Figure 3.2 shows how well the model describes the neutrino oscillation experimental data for the case of NH of neutrino masses. The color bar represents the value of χ^2 ranging from 1 to 30. The best-fit values of the neutrino oscillation parameters obtained from the model are summarized in Table 3.3. The parameters $\sin^2\theta_{12}$, $\sin^2\theta_{23}$, $\sin^2\theta_{13}$ and the two mass-squared differences have best-fit values which fall within the

[2]In our analysis we have accepted only the points that satisfy $\chi^2 \leq 30$, hence, no further analysis is done for the case of IH.

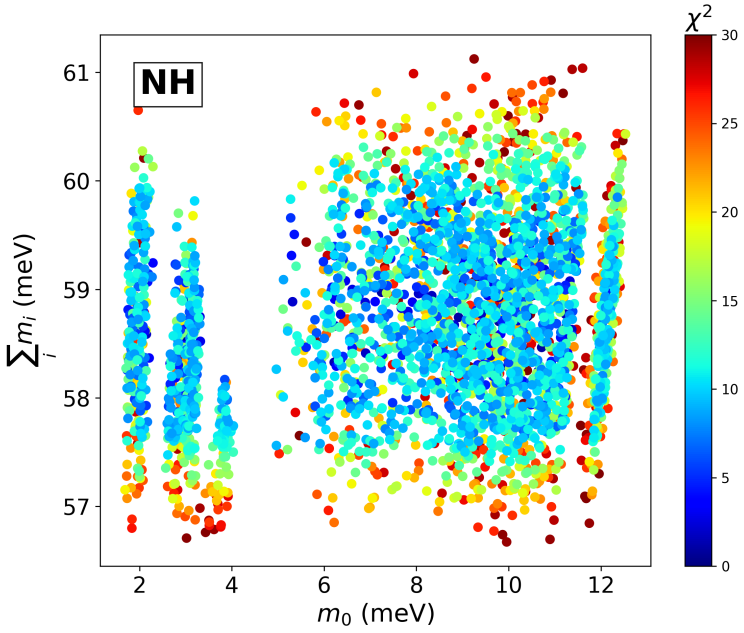

Figure 3.3: Range of values for the mass scale, m_0 and the sum of light neutrino masses, $\sum_i m_i$.

1σ range of experimental values shown in Table 3.2. The value of the Dirac CP-violating phase δ_{CP} corresponding to the χ^2_{min} value is 370.078°, which is within the 3σ range of neutrino oscillation data. The model presented in the previous section offers a reasonable explanation of the most recent experimental data. Its prediction regarding δ_{CP} can be put to the test in forthcoming precision experiments. In Figure 3.3 we present the sum of neutrino masses as a function of the mass scale, m_0 which effectively influences the absolute neutrino masses. There is a cosmological upper bound on the sum of the light neutrino masses, $\sum_i m_i <$ 0.12 eV [47–50] and our model shows a consistent value ranging from 56.67 to 61.12 meV. The effective Majorana neutrino mass $|\langle m_{ee}\rangle|$ that characterizes the process of neutrino-less double beta decay ($0\nu\beta\beta$) is given by

$$|\langle m_{ee}\rangle| = |\sum_i m_i U_{ei}^2| = |c_{12}^2 c_{13}^2 m_1 e^{i\alpha_M} + s_{12}^2 c_{13}^2 m_2 e^{i\beta_M} + s_{13}^2 e^{-2i\delta_{CP}}| = |(m_\nu)_{11}| \tag{3.17}$$

From equation (3.17) we can see that the effective Majorana neutrino mass de-

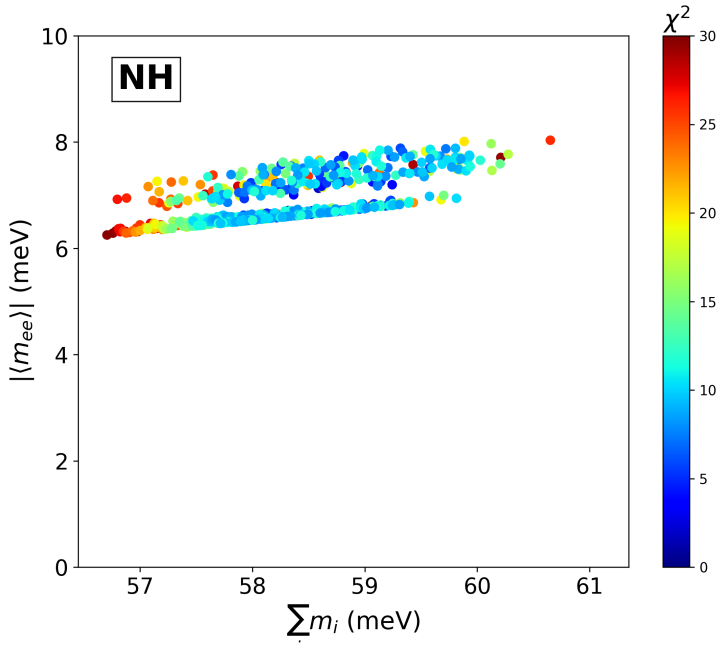

Figure 3.4: The effective Majorana electron neutrino mass, $|\langle m_{ee}\rangle|$ as a function of the sum of light neutrino masses, $\sum_i m_i$.

pends on the Majorana phases as well as the Dirac CP phase and can be given as the (1, 1) element of the neutrino mass matrix of equation (3.8). We used the parameter space illustrated in Figure 3.1 to assess the magnitude of $|\langle m_{ee}\rangle|$. Our findings are presented in Figure 3.4, where it can be seen that the predicted values of $|\langle m_{ee}\rangle|$ fall within the range of 6.25-8 meV. This value is significantly lower than the sensitivity limit of $0\nu\beta\beta$ experiments.

3.4 Conclusion

In this chapter we examined the minimal form of the inverse seesaw model ISS(2, 2) with S_4 flavour symmetry. The S_4 flavour symmetry helps determine the structure of the mass matrices and the mixing pattern in the leptonic sector. We performed a test and studied how well the model describes the experimental data using χ^2 analysis. We found that the model describes the experimental neutrino data for

NH of neutrino masses with the best-fit value at $\chi^2_{min} \approx 0.24$. The model, however, rules out the case of IH of neutrino masses, with $\chi^2_{min} > 100$. The prediction of the Dirac CP phase at the best-fit point is $\delta_{CP} \approx 370.087^\circ$ which can be tested in future precision experiments. Prediction of the model on effective Majorana neutrino mass is also made. The points in the parameter space that satisfy $\chi^2 \leq 30$ have been considered the allowed region for the model parameters. Using this allowed region of the model parameters we evaluate the effective Majorana neutrino mass and found that the obtained values are very small to be tested in future experiments. Experiments such as T2K and NOνA can resolve the octant of the mixing angle θ_{23} and give a precision measurement on Dirac CP-violating phase δ_{CP}, which will help us validate our model. Further, the constrained parameter space obtained from our model may be used to study low-scale leptogenesis and is left for future work.

Bibliography

[1] Adamson, P. *et al.* Improved search for muon-neutrino to electron-neutrino oscillations in MINOS. *Physical Review Letters* **107**, 181802, 2011.

[2] Abe, K. *et al.* Indication of electron neutrino appearance from an accelerator-produced off-axis muon neutrino beam. *Physical Review Letters* **107**, 041801, 2011.

[3] An, F. P. *et al.* Observation of electron-antineutrino disappearance at Daya Bay. *Physical Review Letters* **108**, 171803, 2012.

[4] Ahn, J. K. *et al.* Observation of reactor electron antineutrinos disappearance in the RENO experiment. *Physical Review Letters* **108**, 191802, 2012.

[5] Mohapatra, R. N. & Senjanović, G. Neutrino mass and spontaneous parity nonconservation. *Physical Review Letters* **44** (14), 912, 1980.

[6] Mohapatra, R. N. & Senjanović, G. Neutrino masses and mixings in

gauge models with spontaneous parity violation. *Physical Review D* **23** (1), 165, 1981.

[7] Minkowski, P. $\mu \to e\gamma$ at a rate of one out of 109 muon decays? *Physics Letters B* **67** (4), 421–428, 1977.

[8] Yanagida, T. Horizontal symmetry and masses of neutrinos. *Progress of Theoretical Physics* **64** (3), 1103–1105, 1980.

[9] Mohapatra, R. N. & Valle, J. W. Neutrino mass and baryon-number nonconservation in superstring models. *Physical Review D* **34** (5), 1642, 1986.

[10] Ma, E. Verifiable radiative seesaw mechanism of neutrino mass and dark matter. *Physical Review D* **73** (7), 077301, 2006.

[11] Ma, E. *et al.* Light sterile neutrinos from large extra dimensions. *Physics Letters B* **495** (3-4), 363–368, 2000.

[12] Arkani-Hamed, N. *et al.* Neutrino masses from large extra dimensions. *Physical Review D* **65** (2), 024032, 2001.

[13] González-Garciá, M. C. *et al.* Isosinglet-neutral heavy-lepton production in Z-decays and neutrino mass. *Nuclear Physics B* **342** (1), 108–126, 1990.

[14] Deppisch, F. & Valle, J. Enhanced lepton flavor violation in the supersymmetric inverse seesaw model. *Physical Review D* **72** (3), 036001, 2005.

[15] Morisi, S. & Valle, J. W. Neutrino masses and mixing: a flavour symmetry roadmap. *Progress in Physics* **61** (4-5), 466–492, 2013.

[16] King, S. F. & Luhn, C. Neutrino mass and mixing with discrete symmetry. *Reports on Progress in Physics* **76** (5), 056201, 2013.

[17] King, S. Unified models of neutrinos, flavour and CP violation. *Progress in Particle and Nuclear Physics* **94**, 217–256, 2017.

[18] Brahmachari, B. *et al.* A_4 flavor symmetry and neutrino phenomenology. *Physical Review D* **77** (7), 073008, 2008.

[19] Altarelli, G. & Feruglio, F. Discrete flavor symmetries and models of neutrino mixing. *Reviews of Modern Physics* **82** (3), 2701, 2010.

[20] Lei, M. & Wells, J. D. Minimally modified A_4 Altarelli-Feruglio model for neutrino masses and mixings and its experimental consequences. *Physical Review D* **102** (1), 016023, 2020.

[21] Barman, A. *et al.* Nonzero θ_{13}, CP-violation and neutrinoless double beta decay for neutrino mixing in the $A_4 \times Z_2 \times Z_3$ flavor symmetry model. *International Journal of Modern Physics A* **38** (2), 2350012, 2023.

[22] Vien, V. V. & Long, H. N. Neutrino mixing with nonzero θ_{13} and CP violation in the 3-3-1 model based on A_4 flavor symmetry. *International Journal of Modern Physics A* **30** (21), 1550117, 2015.

[23] Vien, V. Cobimaximal neutrino mixing in the $U(1)_{B-L}$ extension with A_4 symmetry. *Modern Physics Letters A* **35** (38), 2050311, 2020.

[24] Vien, V. B-L model with $A_4 \times Z_3 \times Z_4$ symmetry for 3+1 active-sterile neutrino mixing. *Journal of Physics G: Nuclear and Particle Physics* **49** (8), 085001, 2022.

[25] Vien, V. & Long, H. A_4-based model with linear seesaw scheme for lepton mass and mixing. *Physica Scripta* **98** (1), 015301, 2022.

[26] Mohapatra, R. N. *et al.* High scale mixing unification and large neutrino mixing angles. *Physical Review D* **69** (5), 053007, 2004.

[27] Hagedorn, C. *et al.* S_4 flavor symmetry and fermion masses: towards a grand unified theory of flavor. *Journal of High Energy Physics* **2006** (06), 042, 2006.

[28] Cai, Y. & Yu, H.-B. SO(10) grand unification model with S_4 flavor symmetry. *Physical Review D* **74** (11), 115005, 2006.

[29] Bazzocchi, F. & Morisi, S. S_4 as a natural flavor symmetry for lepton mixing. *Physical Review D* **80** (9), 096005, 2009.

[30] Yang, R.-Z. & Zhang, H. Minimal seesaw model with S_4 flavor symmetry. *Physics Letters B* **700** (5), 316–321, 2011.

[31] Bazzocchi, F. & Merlo, L. Neutrino mixings and the S_4 discrete flavour symmetry. *Progress in Physics* **61** (4-5), 571–596, 2013.

[32] Penedo, J. *et al.* Neutrino mixing and leptonic CP violation from S_4 flavour and generalised CP symmetries. *Journal of High Energy Physics* **2017** (12), 1–57, 2017.

[33] Thapa, B. & Francis, N. K. Resonant leptogenesis and TM_1 mixing in minimal Type-I seesaw model with S_4 symmetry. *European Physical Journal C* **81**, 1–8, 2021.

[34] Dong, P. *et al.* The 3-3-1 model with S_4 flavor symmetry. *The European Physical Journal C* **71** (2), 1544, 2011.

[35] Vien, V. & Long, H. A new flavor symmetry in 3-3-1 model with neutral fermions. *Advances in High Energy Physics* **2014**, 2014.

[36] Vien, V. Lepton mass and mixing in a neutrino mass model based on S_4 flavor symmetry. *International Journal of Modern Physics A* **31** (09), 1650039, 2016.

[37] Vien, V. *et al.* Fermion mass and mixing in a low-scale seesaw model based on the S_4 flavor symmetry. *Progress of Theoretical and Experimental Physics* **2019** (11), 113B04, 2019.

[38] Vien, V. & Long, H. Multiscalar B-L extension based on S_4 flavor symmetry for neutrino masses and mixing. *Chinese Physics C* **45** (4), 043112, 2021.

[39] Vien, V. Renormalizable standard model extension with S_4 symmetry for neutrino mass and mixing. *Canadian Journal of Physics* (ja), 2022.

[40] Ding, G.-J. *et al.* Golden ratio neutrino mixing and A_5 flavor symmetry. *Nuclear Physics B* **857** (3), 219–253, 2012.

[41] Ballett, P. *et al.* Mixing angle and phase correlations from A_5 with generalized CP and their prospects for discovery. *Physical Review D* **92** (9), 093008, 2015.

[42] Abada, A. & Lucente, M. Looking for the minimal inverse seesaw realisation. *Nuclear Physics B* **885**, 651–678, 2014.

[43] Zhao, Z.-h. Realizing tri-bimaximal mixing in minimal seesaw model with S_4 family symmetry. *Physics Letters B* **701** (5), 609–613, 2011.

[44] Esteban, I. *et al.* The fate of hints: updated global analysis of three-flavor neutrino oscillations. *Journal of High Energy Physics* **2020** (9), 1–22, 2020.

[45] Xing, Z.-z. & Zhou, Y.-L. A generic diagonalization of the 3×3 neutrino mass matrix and its implications on the μ–τ flavor symmetry and maximal CP violation. *Phys. Lett. B* **693** (5), 584–590, 2010.

[46] Feroz, F. *et al.* MultiNest: an efficient and robust bayesian inference tool for cosmology and particle physics. *Monthly Notices of the Royal Astronomical Society* **398** (4), 1601–1614, 2009.

[47] Vagnozzi, S. *et al.* Unveiling ν secrets with cosmological data: Neutrino masses and mass hierarchy. *Physical Review D* **96**, 123503, 2017.

[48] Giusarma, E. *et al.* Scale-dependent galaxy bias, CMB lensing-galaxy cross-correlation, and neutrino masses. *Physical Review D* **98**, 123526, 2018.

[49] Tanseri, I. *et al.* Updated neutrino mass constraints from galaxy clustering and CMB lensing-galaxy cross-correlation measurements. *Journal of High Energy Astrophysics* **36**, 1–26, 2022.

[50] Aghanim, N. *et al.* Planck 2018 results-VI. cosmological parameters. *Astronomy & Astrophysics* **641**, A6, 2020.